arXiv:1610.02733v1 [cond-mat.soft] 9 Oct 2016

An improved dissipative coupling scheme for a system of Molecular Dynamics particles interacting with a Lattice Boltzmann fluid

Nikita Tretyakov[a,*], Burkhard Dünweg[a,b,c]

[a] *Max-Planck-Institut für Polymerforschung, Ackermannweg 10, 55128 Mainz, Germany*
[b] *Institut für Festkörperphysik, Technische Universität, Hochschulstraße 12, 64289 Darmstadt, Germany*
[c] *Department of Chemical Engineering, Monash University, Clayton, Victoria 3800, Australia*

Abstract

We consider the dissipative coupling between a stochastic Lattice Boltzmann (LB) fluid and a particle-based Molecular Dynamics (MD) system, as it was first introduced by Ahlrichs and Dünweg (J. Chem. Phys. 111 (1999) 8225). The fluid velocity at the position of a particle is determined by interpolation, such that a Stokes friction force gives rise to an exchange of momentum between the particle and the surrounding fluid nodes. For efficiency reasons, the LB time step is chosen as a multiple of the MD time step, such that the MD system is updated more frequently than the LB fluid. In this situation, there are different ways to implement the coupling: Either the fluid velocity at the surrounding nodes is only updated every LB time step, or it is updated every MD step. It is demonstrated that the latter choice, which enforces momentum conservation on a significantly shorter time scale, is clearly superior in terms of stability and accuracy, and nevertheless only marginally slower in terms of execution speed. The second variant is therefore the recommended implementation.

Keywords: Lattice Boltzmann, Molecular Dynamics, fluid-particle coupling

1. Introduction

In the last decades the Lattice Boltzmann (LB) technique [1, 2, 3, 4, 5] has evolved into a well-founded and efficient numerical tool for the study of fluid mechanics. It has numerous applications, ranging from the studies of turbulence [6] and other macroscopic fluid dynamics problems [7] to soft matter investigations on the meso- or microscale. Hydrodynamics of soft matter is in itself a large field, and LB has been applied to, e. g., liquid crystals [8], two-phase

*Corresponding author
Email address: tretyakov@mpip-mainz.mpg.de (Nikita Tretyakov)

flows [9], binary mixtures [10], and hybrid simulations of particle-based systems, like colloids or polymers, in a solvent. The present paper is a methodological investigation dealing with this last application, which is based upon coupling LB to Molecular Dynamics (MD). This method, which will be referred to by LB/MD, has been described in detail in Ref. [4].

In colloidal dispersions or polymer solutions the molecular structure of the solvent is often irrelevant, while dynamic correlations between the dispersed particles, transmitted via fast momentum transport through the solvent (the so-called "hydrodynamic interactions") are of paramount importance. There are many ways to take these correlations into account in a simulation, of which LB/MD is only one. Competing approaches are Brownian Dynamics (BD) [11], Dissipative Particle Dynamics (DPD) [12], Multi-Particle Collision Dynamics (MPCD) [13], Smoothed Dissipative Particle Dynamics (SDPD) [14], and "conventional" Navier-Stokes equation (NSE) solvers [15]. All these methods have advantages and disadvantages, and these have (at least partly) been discussed in Ref. [4]. Important criteria that a simulation method should satisfy are: (i) consistent representation of thermal fluctuations, which are very important on the small length scales of soft matter (satisfied by all); (ii) linear scaling (satisfied by all except BD); and (iii) control over the amplitude of thermal fluctuations which should depend on the degree of coarse-graining (or the length-scale resolution) of the simulation (satisfied only by LB/MD, SDPD, and NSE). LB/MD is particularly attractive for several reasons: (i) due to the lattice, LB is based on a tight data structure, which allows efficient memory management; (ii) due to the streaming-and-collision structure of the algorithm, the method exhibits a high degree of locality, which makes it amenable to parallelization based upon geometric domain decomposition. Indeed, in a comparative study LB/MD was found to be significantly faster than a DPD simulation of the same physical system [16]. A disadvantage of lattice methods is however their inability to deal with difficult boundary conditions, in particular in cases where these involve a deforming simulation cell [17].

It is clear that LB/MD soft-matter simulations have to take care of two aspects that are foreign to the plain LB method, which is essentially not much more than a NSE solver: On the one hand, one has to introduce thermal fluctuations by means of a suitable stochastic collision operator, and on the other hand, one needs a suitable coupling scheme for interaction with the particle-based system. The first aspect has seen significant progress in the last two decades [18, 19, 20, 21, 22, 23], and this topic shall not be our concern here. For the coupling, various schemes have been developed. Among the most prominent methods, one can mention reflecting boundary conditions [18, 19, 24, 4], force coupling [25, 4], the immersed boundary method (IBM) [26] and external boundary forces (EBF) [27].

The EBF method is applied to extended objects to satisfy a no-slip boundary condition on their surface. The IBM represents a fluid-particle interface by a set of Lagrangian nodes and interactions are applied as body forces to the fluid. These approaches result in a fairly accurate representation of hydrodynamic boundary conditions, however at the expense of a somewhat complicated

algorithm. On the other hand, many soft-matter systems involve objects that are quite large and very "soft" (like polymers of various molecular architectures, tethered membranes, etc.). For these systems the details of the coupling on the local (or monomer) scale do not matter very much — it is only important that the hydrodynamic interactions are correctly represented on larger scales (larger than the monomer size but still significantly smaller than the size of the object as a whole). Therefore, a very simple coupling scheme is desirable, and the force coupling originally put forward by Ahlrichs and Dünweg [25] and recently refined by Schiller [28] satisfies this criterion. It is also clear that Ladd's reflecting boundary method [18, 19] is not suitable for polymer systems, since this would require to model each monomer as an extended sphere, which would be computationally much more expensive than the point-particle representation used in force coupling. It is this latter method upon which we will focus in the present paper.

The force coupling algorithm is inherently dissipative, i. e. the velocity of an MD particle is damped with respect to the velocity of the LB fluid interpolated to the particle's position. Random forces are added to the particles to account for thermal noise. It should be noted that the fluctuation-dissipation theorem stipulates that every dissipation mechanism needs to be compensated by a corresponding noise. This means not only that the viscous damping within the LB fluid must be compensated by a stochastic collision operator, but also that the damping of the particles relative to the surrounding flow needs a compensating noise as well. The counterparts of the coupling forces (damping plus noise) are exerted on the LB fluid to conserve the total momentum. The calculation of the coupling forces takes place every MD step, but the LB update typically needs to be done only after several MD steps. This scheme allows us to capture the dynamics of the fluid and the immersed particles correctly and reproduce hydrodynamic behavior. However, the MD and LB timesteps have to be chosen wisely to find a compromise between the performance and the heat-up of the particle-based system at moderate friction coefficients, which must be viewed as a discretization error. It turns out that the details of this momentum exchange have a significant influence on the size of the discretization error, and the topic of the present investigation is to improve the method with respect to this aspect.

A naive and straightforward approach would involve a re-calculation of the streaming velocities at the surrounding LB nodes only every LB step. In the present paper, we investigate both this method as well as a refined one, where the streaming velocities at the surrounding nodes are rather re-calculated every MD time step, in accord with the coupling forces. This latter scheme is obviously more accurate, and gives conservation of total momentum not only on the scale of the LB time step, but rather of the MD time step. We also find that this improves the stability of the simulation substantially, and permits more freedom in the choice of the MD and LB time steps. Furthermore, the computational overhead associated with the improved scheme is insignificant, since it employs already available momentum changes and only adds a few more operations on the surrounding lattice sites.

The paper is organized as follows: Sec. 2 presents a short overview of the

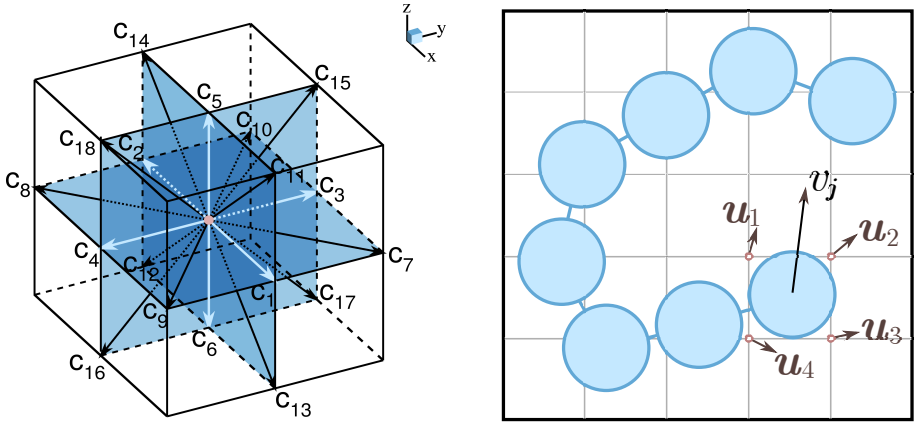

(a) (b)

Figure 1: (a) D3Q19 scheme with 19 velocities connecting a chosen lattice site with its neighbors. (b) Schematic representation of the LB to MD coupling.

LB method. The details on the coupling technique and the update scheme are given in Sec. 3, together with a comparison between the two strategies mentioned above. We conclude in Sec. 4 with a short summary.

2. Lattice Boltzmann technique

In this section we provide a brief explanation of the LB method. For details and the underlying theory, we refer the reader to the review given in Ref. [4].

The LB scheme can be viewed as a version of coarse-graining of the solvent fluid: Instead of explicit consideration of solvent molecules and their degrees of freedom, the LB method deals with a set of so-called populations $f_i(\vec{r}, t)$ on every lattice site $\vec{r}$ at time t. The population f_i is a quantity proportional to the number of fluid particles flowing with a specific velocity, locally at position $\vec{r}$ at time t. Typically, f_i is interpreted as the local mass density associated with the lattice velocity $\vec{c}_i$. The finite set of velocities is chosen such that in one time step neighboring lattice sites are connected. The most popular model in three dimensions is called D3Q19. It has 19 velocity vectors $\vec{c}_i$ (including $\vec{c}_0 = 0$), and is schematically shown in Fig. 1a.

The hydrodynamic quantities of the fluid are found by evaluating moments of the populations with respect to discrete velocity set: The mass density and the mass density flux (or momentum density) at the lattice site $\vec{r}$ are given by

$$\rho(\vec{r}) = \sum_i f_i \tag{1}$$

and

$$\vec{j}(\vec{r}) = \rho(\vec{r})\vec{u}(\vec{r}) = \sum_i f_i \vec{c}_i, \tag{2}$$

respectively. This also defines the local flow velocity $\vec{u}$.

The change of the populations during one LB timestep Δt_{LB} on a lattice site is summarized by the Lattice Boltzmann equation (LBE):

$$f_i(\vec{r} + \vec{c}_i \Delta t_{\mathrm{LB}}, t + \Delta t_{\mathrm{LB}}) = f_i(\vec{r}, t) + \Delta_i, \tag{3}$$

where Δ_i is the so-called collision operator. The choice of the collision operator is dictated by (i) conservation of mass and momentum, (ii) the rate of stress relaxation in the framework of a linearized Boltzmann equation, which determines the viscosities, (iii) proper implementation of the thermal fluctuations, and (iv) external forces (for example, friction forces from the MD particles, which are the main concern of the present paper). A very general formulation is the multiple-relaxation times (MRT) collision operator [29], as discussed in Ref. [21]. After the collision step, the post-collision populations are propagated to the neighboring sites according to the velocity vectors $\vec{c}_i$. This is again relatively easy to parallelize. As long as the immersed particles are absent, or present only at a low concentration, such that their contribution to the overall numerical effort is insignificant, load-balancing problems do not occur. For details, see Ref. [4].

3. Coupling algorithm

The force coupling scheme is sketched in Fig. 1b. The force $\vec{F}_j$ acting on MD particle number j, which is located at position $\vec{R}_j$ and moves with velocity $\vec{v}_j$, is given by

$$\vec{F}_j = \vec{F}_j^{\mathrm{cons}} - \zeta \left[\vec{v}_j - \vec{u}(\vec{R}_j) \right] + \vec{F}_j^{\mathrm{rand}}, \tag{4}$$

where $\vec{F}_j^{\mathrm{cons}}$ is the total conservative force on the particle, resulting from all interactions with other particles. It has no relation to the LB fluid and we will therefore omit it from now on in the text. The last term $\vec{F}_j^{\mathrm{rand}}$ is the random force due to thermal motion. The second term is the frictional force due to the coupling, where ζ is the particle's friction coefficient (here, for simplicity, assumed to be identical for all particles), while the term in brackets is the velocity of the particle $\vec{v}_j$ relative to the fluid velocity $\vec{u}$ at the particle's position $\vec{R}_j$. Since the fluid velocity is only defined at the lattice sites, one has to interpolate $\vec{u}(\vec{R}_j)$ from the velocities at some neighboring sites. A simple interpolation scheme involves (in 3D) eight sites $\vec{r} = \vec{r}_k$, $k = 1, \ldots, 8$, which form the cube that contains the particle:

$$\vec{u}(\vec{R}_j) = \sum_{k=1}^{8} \delta_k \, \vec{u}(\vec{r}_k), \tag{5}$$

where δ_k are weights based on the distances (in x, y and z direction) between $\vec{R}_j$ and the sites $\vec{r}_k$. Clearly, within one MD time step Δt, the particle's coupling to the fluid results in a change of its momentum by an amount $\Delta \vec{P}_j$. We here

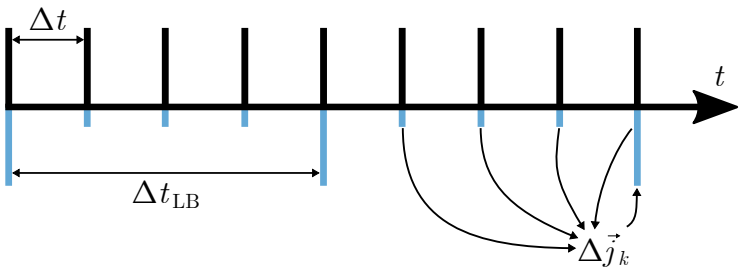

Figure 2: Schematic representation of the LB and MD timescales.

consider only a very simple integration scheme, which evaluates the momentum change via

$$\Delta \vec{P}_j = \Delta t \left\{ -\zeta \left[\vec{v}_j - \vec{u}(\vec{R}_j) \right] + \vec{F}_j^{\mathrm{rand}} \right\}, \tag{6}$$

where we take $\vec{R}_j$, $\vec{v}_j$, and $\vec{F}_j^{\mathrm{rand}}$ as the values obtained or generated at the beginning of the MD step.

To conserve momentum one has to consider Newton's third law and account for the force exerted by the particle j onto the surrounding LB fluid. In other words, the total momentum of the fluid has to be changed by the amount $-\Delta \vec{P}_j$, and locality dictates that this amount of momentum should be distributed onto some surrounding sites, again with some interpolation scheme. Not surprisingly, one should use the *same* interpolation scheme as the method that is used for the interpolation of the velocities; analysis of the continuum version of the algorithm shows that this is necessary in order to satisfy the fluctuation-dissipation relation [4]. Furthermore, we can transform the change in momentum at the site $\vec{r}_k$ to a force density, which is thus found to be

$$\vec{f}_k = -\frac{1}{\Delta t\, a^3} \delta_k \Delta \vec{P}_j, \tag{7}$$

where a is the lattice spacing. Now, the problem how to apply a force density in LB has a nice and well-defined solution [4] first reported by Guo et al. [30]: The force density $\vec{f}_k$ gives rise to a certain contribution Δ_i' to the collision operator, which is linear in $\vec{f}_k$ and which is adjusted in such a way that not only the momentum transfer is correct, but also the continuum limit obtained via a second-order Chapman-Enskog expansion [4] is just the NSE without any spurious terms. It should be noted that Δ_i' depends not only on $\vec{f}_k$ but also on the local streaming velocity $\vec{u}$.

However, due to the fact that typically Δt is smaller than Δt_{LB}, as a result of the coarse-graining of the LB fluid with respect to time [25], the question remains open how to implement this precisely. In what follows, we will discuss the method in terms of the change in momentum density corresponding to the time Δt,

$$\Delta \vec{j}_k = \vec{f}_k \, \Delta t. \tag{8}$$

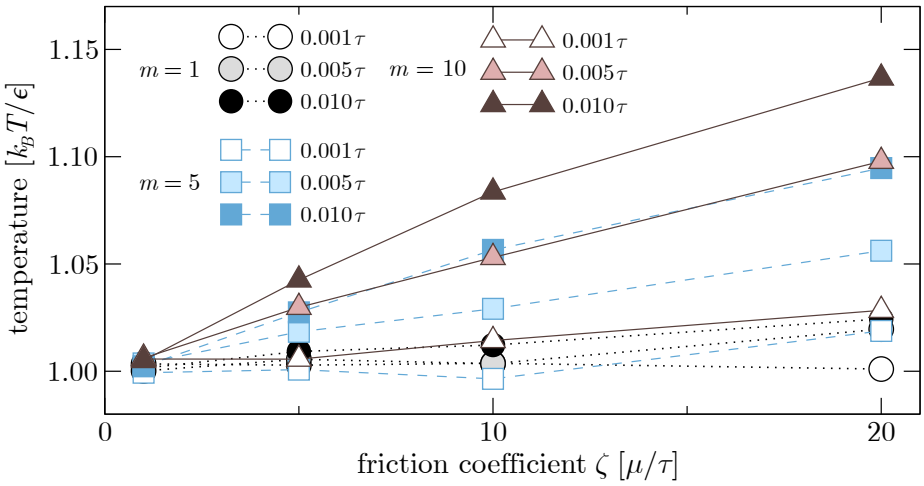

Figure 3: Temperature of the particle-based system as a function of the friction coefficient ζ for variant A coupling. The data for time-scale contrasts of $m = 1$, 5 and 10 are plotted in black, blue and brown, respectively. The shading of the symbols (from open to full) corresponds to MD time steps of $0.001\,\tau$, $0.005\,\tau$ and $0.010\,\tau$.

We denote the ratio between the two time steps by $m = \Delta t_{\mathrm{LB}}/\Delta t$. In order to keep the coupled simulations synchronized, it is necessary that m is an integer; typically we will have $m > 1$. The situation that then arises is schematically depicted in Fig. 2.

The coupling force $\vec{F}_j$ is computed every MD time step (black vertical lines) and employed to integrate the equation of motion of particle j. At the same time, the concomitant changes in momentum density, $\Delta\vec{j}_k$, are made known to their respective LB nodes $\vec{r}_k$. The simplest method (which we will call variant A in what follows) would then accumulate these values for m steps, while keeping the populations and streaming velocities on the surrounding sites fixed. This is indicated in Fig. 2 by black arrows. After these m steps, the collision operator (with Δ_i' corresponding to the total time Δt_{LB}) is applied, followed by the streaming step (long blue vertical lines).

It is desirable to make m as large as possible, in order to avoid the CPU-intensive LB steps as much as possible. This is essential for the computational performance of most physical applications. The more dilute the solution is, the larger is the CPU time fraction of the LB part. For a typical semidilute polymer solution (where the monomer volume fraction is small) we observe that the integration of the equations of motion of the particle-based system takes less than 5% of the total time. Therefore, the ability to reduce the number of LB collision-streaming steps speeds up the simulations considerably.

The described coupling scheme is simple and therefore computationally efficient. It is also reasonably robust in a moderate range of parameters. To test this, we have calculated the average temperature of the particle-based system, evaluated by the mean kinetic energy. The particle system consists of

ten bead-spring polymer chains with 256 beads each, whose interactions are given by the standard Kremer-Grest model [31]. All monomers interact via a Lennard-Jones (LJ) potential with energy parameter ϵ and length parameter σ, where the interaction is however not cut off at $2^{1/6}\sigma$, but rather at $2^{7/6}\sigma$. Furthermore, the monomers are connected by FENE springs, as in the standard model. The monomers have a mass μ, and τ is the standard Lennard-Jones time $\tau = \left(\mu\sigma^2/\epsilon\right)^{1/2}$. The size of the simulation box is $(20\sigma)^3$. The LB lattice spacing is set to $a = \sigma$, and the fluid density is $\rho = 1.0\mu/a^3$. The desired temperature of the system is $k_\mathrm{B}T = 1.0\epsilon$, and the fluid shear viscosity is $\eta = 3\epsilon\tau/\sigma^3$.

The result of the test is shown in Fig. 3. For some parameters, we observe significant deviations between the "measured" temperature and its desired input value. At fixed m, we find that the deviations decrease systematically when the time step is decreased, and therefore we interpret this behavior as a discretization error. Furthermore, the deviations also increase systematically with the friction constant ζ. At small friction coefficients ($\zeta \leq 5\,\mu/\tau$), moderate MD timesteps ($\Delta t \leq 0.005\,\tau$) and moderate time-scale contrasts ($m \leq 5$) the deviations do not exceed 3% (cf. half-shaded squares in Fig. 3). However, outside the above mentioned parameter region (especially for larger time-scale contrasts) the MD system is significantly heated up. The deviations can be as large as 15% (cf. full shaded triangles in Fig. 3). It is interesting to notice that the heat-up at fixed LB time step is the same (cf. the systems at $m = 5$ and $\Delta t = 0.010\tau$ *vs.* $m = 10$ and $\Delta t = 0.005\tau$).

The origin of these errors lies in the nature of the coupling: The frictional force acting on every particle is calculated every MD step, but for determining the reference velocity $\vec{u}(\vec{R}_j)$ variant A uses the streaming velocities on the sites $\vec{r}_k$ that have been calculated at the last LB update at time $t_\mathrm{LB}^\mathrm{last}$ (long blue vertical lines in Fig. 2). We therefore modify variant A to a more accurate scheme (variant B) where the MD-LB coupling is done every MD time step, such that the time lag of the reference velocity is substantially reduced (short and long blue vertical lines in Fig. 2). More precisely, the scheme proceeds as follows: At time $t = t_\mathrm{LB}^\mathrm{last}$ we apply the collision operator corresponding to MRT relaxation and to thermal noise applied to the fluid, plus Δ_i' corresponding to the total accumulated momentum transfer from the particles (on the time scale Δt_LB). We also perform an LB streaming step. At time $t = t_\mathrm{LB}^\mathrm{last} + \Delta t$, we first apply thermal noise to the particle. After this the friction force is calculated, using the "old" lattice velocities obtained at $t = t_\mathrm{LB}^\mathrm{last}$. These forces are used to update the particle positions and momenta by means of the MD integrator (typically we use a velocity Verlet scheme). At the same time, these thermal and frictional forces alter the momentum density on the neighboring fluid sites by $\Delta\vec{j}_k$. This in turn is used to update the lattice velocities on the surrounding sites $\vec{r}_k$. After that we can apply the same procedure at time $t = t_\mathrm{LB}^\mathrm{last} + 2\Delta t$, where now the lattice velocities from the time $t = t_\mathrm{LB}^\mathrm{last} + \Delta t$ are used to calculate the friction force. The scheme is then continued for all together m times, until at time $t = t_\mathrm{LB}^\mathrm{last} + \Delta t_\mathrm{LB}$ we again perform a full LB update. The overall momentum conservation then holds at every single MD time step, and not only at every

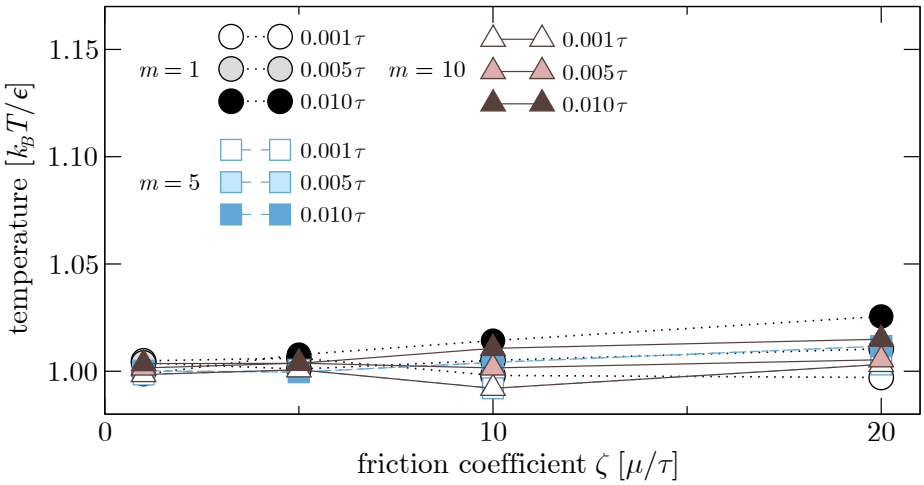

Figure 4: Same as Figure 3 but for variant B coupling.

LB time step as in variant A. One should thus expect that variant B, via the reduction of the time lag between the particle velocity and the lattice velocities at the nearby nodes, will allow substantially larger time-scale contrasts, and thus more efficient simulations.

The effect that the improved coupling scheme has is enormous and can be seen in detail in Fig. 4. Even when the time-scale contrast is as large as $m = 10$ and the MD time step takes the large value $\Delta t = 0.01\tau$, the difference between the observed and the desired temperature is less than 2%, for all values of ζ that we have studied! It is therefore obvious that variant B is greatly superior to variant A in the correct reproduction of the particle kinetic energy — and this means it has also much more superior stability. This in turn means that one can afford a much larger time-scale contrast, and thus gain enormously in computational efficiency. The programming effort to switch from variant A to variant B is minimal, involving just a few lines of code. Similarly, the additional CPU effort is, at least for dilute systems, also very small, since only a few nodes in the vicinity of the particles are involved.

The variant B of the coupling presented above is a simplification of a more refined approach, which involves a full update of the *populations* (rather than only the momenta) on the lattice sites $\vec{r}_k$ at *every MD time step*. This operation requires neither MRT relaxation nor adding random noise to the LB fluid nor the streaming. The update is done via the collision operator Δ_i' corresponding to the momentum transfer from the particles. Since Δ_i' depends not only on the momentum transfer, but also on the local streaming velocity [4, 30], this is genuinely different from the approach outlined above and involves a small nonlinear correction to the flow velocities: At the next time step the lattice velocities are calculated from the changed populations (and not simply from the momentum transfer) and the update procedure is repeated again. The full

LB update with streaming is done every m time steps as usual. In tests we found that this refinement indeed improves the accuracy of the temperature further, but only by at most a fraction of 20% with respect to the simplified variant B. This virtue however is counterbalanced by a drop of the CPU efficiency by the same amount and a somewhat more cumbersome programming implementation. Therefore we recommend the variant B as a standard coupling scheme for MD particles interacting with an LB fluid.

4. Conclusions

The present study highlights the importance of implementing the force coupling in such a way that it keeps the discretization errors reasonably small, such that large time-scale contrasts (and therefore efficient simulations) can be afforded. This goal is achieved by (i) minimizing the time lag between the particle velocity and the streaming velocities at the nearby nodes, and (ii) enforcing momentum conservation at every single MD time step. At the same time, the computational cost of the modification is negligible, since only quantities are used that are available during the simulation anyway.

In contrast to a straightforward variant A, variant B employs the existing coupling forces stored at the lattice sites to update the velocities of the LB fluid every MD step. Though in variant A the coupling forces are also calculated every MD step, they are merely accumulated until the LB update step. Conversely, variant B proposes to apply the coupling forces to modify the velocities of the LB fluid immediately, thus allowing for a more accurate calculation of the reference velocity that enters the friction force. This fine modification has a dramatic effect on the stability of the simulation: The temperature of the MD system is kept effectively constant in a significantly extended parameter space comprising the friction coefficient of the coupling, the MD timestep and the time-scale contrast between LB and MD.

In the present investigation we relied on a rather simple interpolation scheme to facilitate the coupling. A more sophisticated and accurate approach is to consider several neighboring lattice shells. This, however, comes at the expense of increased computational time. Nevertheless, the difference between variant A and variant B is present regardless of the details of the interpolation. We therefore expect that essentially identical results and conclusions would be obtained for higher-order interpolations as well.

5. Acknowledgments

We thank A. C. Fogarty for a careful reading of the manuscript, and her useful comments. Stimulating discussions with U. Schiller and A. J. C. Ladd are gratefully acknowledged. This work was supported by the DFG Collaborative Research Center TRR 146 “Multiscale Simulation Methods for Soft Matter Systems”.

References

References

[1] S. Succi, The Lattice Boltzmann Equation for Fluid Dynamics and Beyond, Clarendon Press, Oxford, 2001.

[2] R. Benzi, S. Succi, M. Vergassola, The Lattice Boltzmann equation: theory and applications, Physics Reports 222 (3) (1992) 145–197. doi:10.1016/0370-1573(92)90090-M.

[3] Y. H. Qian, D. d'Humieres, P. Lallemand, Lattice BGK Models for Navier-Stokes Equation, Europhysics Letters 17 (6) (1992) 479–484. doi:10.1209/0295-5075/17/6/001.

[4] B. Dünweg, A. J. C. Ladd, Lattice Boltzmann simulations of soft matter systems, in: C. Holm, K. Kremer (Eds.), Advanced Computer Simulation Approaches for Soft Matter Sciences III, Vol. 221 of Advances in Polymer Science, Springer Berlin Heidelberg, 2009, pp. 89–166. doi:10.1007/978-3-540-87706-6_2.

[5] C. K. Aidun, J. R. Clausen, Lattice-Boltzmann method for complex flows, Annual Review of Fluid Mechanics 42 (1) (2010) 439–472. doi:10.1146/annurev-fluid-121108-145519.

[6] H. Yu, S. S. Girimaji, L.-S. Luo, DNS and LES of decaying isotropic turbulence with and without frame rotation using Lattice Boltzmann method, Journal of Computational Physics 209 (2) (2005) 599–616. doi:http://dx.doi.org/10.1016/j.jcp.2005.03.022.

[7] S. Succi, Lattice Boltzmann across scales: from turbulence to DNA translocation, The European Physical Journal B 64 (3) (2008) 471–479. doi:10.1140/epjb/e2008-00067-3.

[8] D. Marenduzzo, E. Orlandini, M. E. Cates, J. M. Yeomans, Steady-state hydrodynamic instabilities of active liquid crystals: Hybrid Lattice Boltzmann simulations, Physical Review E 76 (2007) 031921. doi:10.1103/PhysRevE.76.031921.

[9] M. R. Swift, E. Orlandini, W. R. Osborn, J. M. Yeomans, Lattice Boltzmann simulations of liquid-gas and binary fluid systems, Physical Review E 54 (1996) 5041–5052. doi:10.1103/PhysRevE.54.5041.

[10] V. M. Kendon, M. E. Cates, I. Pagonabarraga, J.-C. Desplat, P. Bladon, Inertial effects in three-dimensional spinodal decomposition of a symmetric binary fluid mixture: a Lattice Boltzmann study, Journal of Fluid Mechanics 440 (2001) 147–203. doi:10.1017/S0022112001004682.

[11] D. L. Ermak, J. A. McCammon, Brownian dynamics with hydrodynamic interactions, The Journal of Chemical Physics 69 (4) (1978) 1352–1360. doi:10.1063/1.436761.

[12] P. Espanol, P. Warren, Statistical Mechanics of Dissipative Particle Dynamics, Europhysics Letters 30 (4) (1995) 191–196. doi:10.1209/0295-5075/30/4/001.

[13] G. Gompper, T. Ihle, D. M. Kroll, R. G. Winkler, Multi-Particle Collision Dynamics: A Particle-Based Mesoscale Simulation Approach to the Hydrodynamics of Complex Fluids, in: C. Holm, K. Kremer (Eds.), Advanced Computer Simulation Approaches for Soft Matter Sciences III, Vol. 221 of Advances in Polymer Science, Springer Berlin Heidelberg, 2009, pp. 1–87. doi:10.1007/978-3-540-87706-6_1.

[14] P. Espanol, M. Revenga, Smoothed dissipative particle dynamics, Physical Review E 67 (2) (2003) 026705. doi:10.1103/PhysRevE.67.026705.

[15] F. Balboa Usabiaga, J. Bell, R. Delgado-Buscalioni, A. Donev, T. Fai, B. Griffith, C. Peskin, Staggered Schemes for Fluctuating Hydrodynamics, Multiscale Modeling & Simulation 10 (4) (2012) 1369–1408. doi:10.1137/120864520.

[16] J. Smiatek, M. Sega, C. Holm, U. D. Schiller, F. Schmid, Mesoscopic simulations of the counterion-induced electro-osmotic flow: A comparative study, The Journal of Chemical Physics 130 (24). doi:10.1063/1.3152844.

[17] A. M. Kraynik, D. A. Reinelt, Extensional motions of spatially periodic lattices, International Journal of Multiphase Flow 18 (6) (1992) 1045–1059. doi:10.1016/0301-9322(92)90074-Q.

[18] A. J. C. Ladd, Numerical simulations of particulate suspensions via a discretized Boltzmann equation. Part 1. Theoretical foundation, Journal of Fluid Mechanics 271 (1994) 285–309. doi:10.1017/S0022112094001771.

[19] A. J. C. Ladd, Numerical simulations of particulate suspensions via a discretized Boltzmann equation. Part 2. Numerical results, Journal of Fluid Mechanics 271 (1994) 311–339. doi:10.1017/S0022112094001783.

[20] R. Adhikari, K. Stratford, M. E. Cates, A. J. Wagner, Fluctuating Lattice Boltzmann, Europhysics Letters 71 (3) (2005) 473–479. doi:10.1209/epl/i2004-10542-5.

[21] B. Dünweg, U. D. Schiller, A. J. C. Ladd, Statistical mechanics of the fluctuating Lattice Boltzmann equation, Physical Review E 76 (2007) 036704. doi:10.1103/PhysRevE.76.036704.

[22] B. Dünweg, U. D. Schiller, A. J. C. Ladd, Progress in the understanding of the fluctuating Lattice Boltzmann equation, Computer Physics Communications 180 (4) (2009) 605–608. doi:10.1016/j.cpc.2009.01.014.

[23] G. Kaehler, A. J. Wagner, Fluctuating ideal-gas Lattice Boltzmann method with fluctuation dissipation theorem for nonvanishing velocities, Physical Review E 87 (6) (2013) 063310. doi:10.1103/PhysRevE.87.063310.

[24] A. J. C. Ladd, R. Verberg, Lattice-Boltzmann simulations of particle-fluid suspensions, Journal of Statistical Physics 104 (5) (2001) 1191–1251. doi:10.1023/A:1010414013942.

[25] P. Ahlrichs, B. Dünweg, Simulation of a single polymer chain in solution by combining Lattice Boltzmann and Molecular Dynamics, The Journal of Chemical Physics 111 (17) (1999) 8225–8239. doi:10.1063/1.480156.

[26] C. S. Peskin, The immersed boundary method, Acta Numerica 11 (2002) 479–517. doi:10.1017/S0962492902000077.

[27] J. Wu, C. K. Aidun, Simulating 3d deformable particle suspensions using Lattice Boltzmann method with discrete external boundary force, International Journal for Numerical Methods in Fluids 62 (2010) 765–783. doi:10.1002/fld.2043.

[28] U. D. Schiller, A unified operator splitting approach for multi-scale fluid-particle coupling in the Lattice Boltzmann method, Computer Physics Communications 185 (10) (2014) 2586–2597. doi:10.1016/j.cpc.2014.06.005.

[29] D. d'Humieres, I. Ginzburg, M. Krafczyk, P. Lallemand, L.-S. Luo, Multiple-relaxation-time Lattice Boltzmann models in three dimensions, Philosophical Transactions: Mathematical, Physical and Engineering Sciences 360 (1792) (2002) 437–451.

[30] Z. Guo, C. Zheng, B. Shi, Discrete lattice effects on the forcing term in the lattice Boltzmann method, Physical Review E 65 (4) (2002) 046308. doi:10.1103/PhysRevE.65.046308.

[31] G. S. Grest, K. Kremer, Molecular Dynamics simulation for polymers in the presence of a heat bath, Physical Review A 33 (1986) 3628–3631. doi:10.1103/PhysRevA.33.3628.